Evidence for Two-Band Superconductivity from Break-Junction Tunneling on MgB_2

H. Schmidt,[1,2] J. F. Zasadzinski,[1,2] K. E. Gray,[1] and D. G. Hinks[1]

[1]*Materials Science Division, Argonne National Laboratory, Argonne, Illinois 60439*
[2]*Physics Division, Illinois Institute of Technology, Chicago, Illinois 60616*
(Received 30 June 2001; published 6 March 2002)

Superconductor-insulator-superconductor tunnel junctions have been fabricated on MgB_2 that display Josephson and quasiparticle currents. These junctions exhibit a gap magnitude, $\Delta \sim 2.5$ meV, that is considerably smaller than the BCS value, but which clearly and reproducibly closes near the bulk T_c. In conjunction with fits of the conductance spectra, these results are interpreted as direct evidence of two-band superconductivity.

The discovery of superconductivity in MgB_2 has led to intense research activity, but the nature of the energy gap, Δ, has been elusive. Tunneling spectroscopy, which is the most direct measure of this quantity, has revealed a large spread of Δ values and considerable variation in its spectral shape. Sharp, BCS-like tunneling spectra have been observed in scanning tunneling microscopy (STM) with a surprisingly small $\Delta = 2.0$ meV [1]. Other STM and point-contact studies revealed double-peaked spectra at low temperatures [2,3] that were interpreted as evidence for two-gap superconductivity. A provocative suggestion is that multiple gaps are a consequence of the coupling of distinct electronic bands [4]. Our ability to fabricate superconductor-insulator-superconductor (SIS) break junctions has led to unique observations and we have gone beyond these initial reports to present more compelling evidence that MgB_2 is one of the rare examples of two-band superconductivity. In addition, our identification of a weak higher-bias spectral feature has provided important insight into the nature of the interband coupling.

The simplicity of the crystalline structure in MgB_2 allows for *ab initio* calculations of its electronic properties [5], from which it is known that the Fermi surface consists of four sheets, two being two dimensional (2D) bonding σ bands and two being three dimensional (3D) bonding and antibonding π bands. An and Pickett [6] propose superconductivity to be driven by the 2D σ bands, where electrons are strongly coupled primarily to the E_{2g} phonon mode. This raises important questions of how superconductivity would manifest itself on the 3D sheets and how the tunneling density of states (DOS) would depend on the crystallographic orientation.

A more recent work [4] treated the problem by reducing it to two distinct bands which, in the clean limit, leads to the appearance of two isotropic gaps, $\Delta_2 \sim 7.2$ meV and $\Delta_1 \sim 2.4$ meV, associated with the 2D and 3D bands, respectively. The small gap, Δ_1, on the 3D sheets is enhanced above its intrinsic value due to virtual phonon exchange (pair transfer) with the 2D sheets and should persist up to the bulk T_c. The results of our tunneling study address these issues in the following ways. First, the small gap feature is *unambiguously* tracked to high temperatures

where it is still visible in the *raw data,* a key observation supporting two-band superconductivity. These junctions probe only the band with the small, induced gap suggesting the *SIS* configuration strongly favors tunneling between the 3D sheets. Second, a subtle spectral feature is observed in the conductance near 9 meV that resembles strong-coupling effects. Using a theoretical, two-band model [7] that treats pair transfer and the quasiparticle self-energy on an equal footing, we have quantitatively fit this feature. This indicates that self-energy effects originating from quasiparticle scattering between bands are important. Finally and importantly, using unique features of *SIS* junctions, we have more rigorously ruled out proximity effects which otherwise can mimic the temperature dependencies and the quasiparticle self-energy effects of two-band superconductivity.

Compact samples of MgB_2 were formed from amorphous B powder (4N's purity) and high purity Mg. The B powder was pressed into pellets under 6 kbar pressure. These freestanding pellets were reacted with Mg vapor at 850 °C for 2 h in a BN container under 50 bars of Ar. During the diffusion reaction the pellets broke up into irregularly shaped pieces several mm on a side. The material typically showed $T_c = 39$ K. To obtain a clean and smooth surface, the samples were polished until a shiny surface was exposed. No solvent was used and the samples were cleaned only in a flow of dry N_2 gas.

The tunneling measurements were performed on two different samples (A and B) using a point-contact apparatus [8] with a gold tip. This technique yielded superconductor-insulator-normal metal (SIN) junctions as well as SIS break junctions, the latter being confirmed by fits to the temperature-dependent conductance as well as the observation of Josephson currents. Figure 1 gives an example of a Josephson tunnel junction obtained on sample A. In the current voltage characteristic there is a distinct jump visible between a well-pronounced, slightly hysteretic Josephson current and the quasiparticle branch which displays a gap feature at $eV = 2\Delta$. In the $\frac{dI}{dV}$ vs V spectra, sharp peaks are seen which can be fit to a BCS s-wave model with $\Delta = 2.1$ meV and $\Gamma = 0.5$ meV. The fit is very good except for a weak spectral feature in the data near 9 mV,
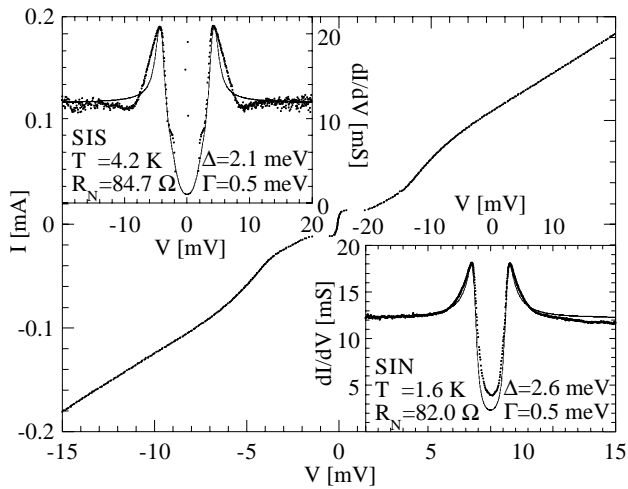
FIG. 1. Josephson tunnel junction on MgB_2 displaying an energy gap of 2.1 meV. Upper inset: *s*-wave fit to the conductance characteristic. Lower inset: Comparison to an *SIN* junction on sample *B* showing a comparable gap magnitude at 1.6 K.

which we discuss later. The simultaneous observation of a well-developed gap feature and a significant Josephson current establishes these junctions to be of *SIS* geometry. The gap value is significantly less than the BCS expectation of 5.9 meV but consistent with the $I_c R_N$ product of 2.2 meV for this junction (other junctions gave comparable values). Note that similarly low values of $I_c R_N$ were found in a recent study of Josephson junctions in MgB_2 [9] prepared by a completely different break-junction method. Although the focus of this study is on the *SIS* junctions, similar gap values were consistently found in *SIN* junctions (lower inset of Fig. 1). Fits to a smeared BCS model yield $\Delta = 2.6$ meV and $\Gamma = 0.5$ meV, which are consistent with the parameters obtained for *SIS* junctions.

Many *SIS* junctions were obtained at different locations on samples *A* and *B*. With increasing resistance of the junction the Josephson currents decrease, and for contact resistances higher than ∼10 kΩ no supercurrent is visible at zero bias. Nevertheless, the junctions could be easily identified as *SIS* by the evolution of the conductance spectra with increasing temperature. *SIN* junctions show a rapid decrease in peak height at $eV = \Delta$ with increasing temperature, while the peak position remains approximately constant. In contrast, the gap structure of *SIS* junctions remains sharp even for elevated temperatures, and the 2Δ-peak position follows the closing of the gap at T_c. We traced three such junctions formed on different parts of the MgB_2 sample *A* up to temperatures of ∼30 K, and two of these sets of data are shown in Fig. 2, while the third is shown as a color map in Fig. 3. What is immediately evident in the raw data is that the small gap persists up to 30 K. Each curve shown in Fig. 2 was divided by R_N (the high bias resistance of the 4.2 K data) and then fit to an *s*-wave gap *SIS* model using the measured temperature. The smearing parameter Γ was adjusted once to reproduce the low-temperature data and
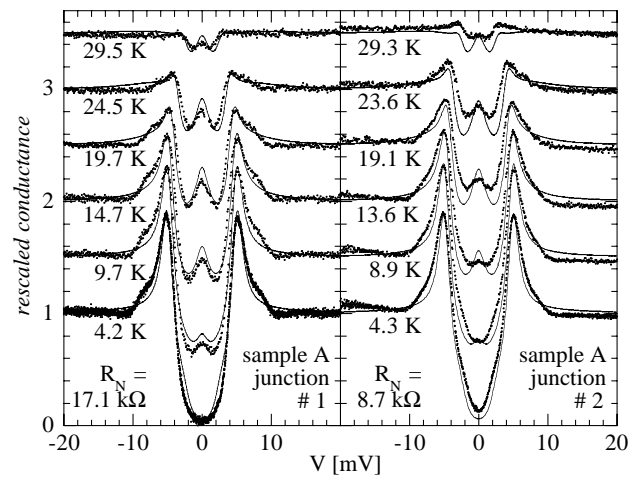

FIG. 2. Temperature dependence of two high-resistance *SIS* tunnel junctions together with *s*-wave fits reproducing all major features of the conductance characteristics, including the evolution of a zero-bias peak due to thermally activated current. Each spectrum is rescaled by the indicated R_N.

then held fixed. This was done to prove the ability of the model to account for all major features of the temperature-dependent data using Δ as the only adjustable parameter. The fits shown in Fig. 2 reproduce the peak heights, the shape of the in-gap conductance, as well as the evolution of the zero-bias peak that is due to thermally activated quasiparticle current. This zero-bias feature cannot appear in *SIN* tunneling but is a known feature of *SIS* tunneling. The magnitude of this central peak is surprisingly high, and this is caused by the unusual case of a small gap which persists to comparatively high temperatures (much higher
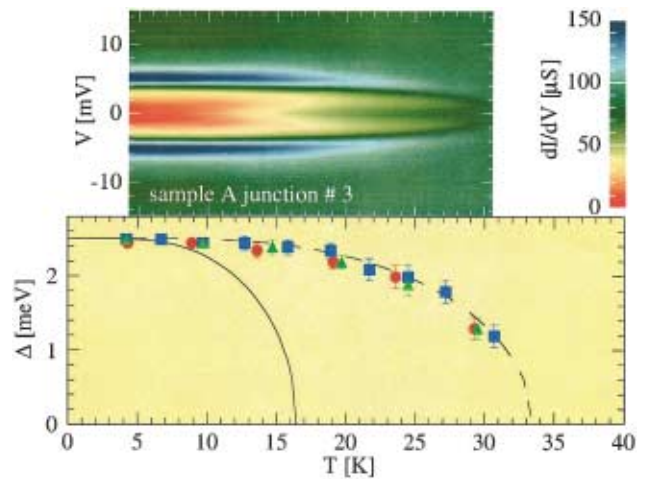

FIG. 3 (color). Top panel: Color map of *SIS* junction conductance spectra as a function of temperature. Bottom panel: Temperature dependence of the small superconducting gap Δ_1. Symbols are data extracted from *SIS* fits to the conductance spectra (different symbols represent three different experiments). The solid line gives $\Delta(T)$ according to BCS theory, using the expected ratio of $2\Delta(0)/k_B T_c$. The dashed line gives a *rescaled* BCS dependence with both Δ and T_c adjusted to fit the experimental data.

than the BCS T_c connected with this gap) thus giving rise to unusually large thermal activation of quasiparticles. The BCS T_c for a low-temperature gap of ~ 2.5 meV is below 17 K, and the gap seen here is still clearly developed at a temperature around 30 K. This rules out a lower T_c on the sample surface as an explanation of the small gap value as this would display a second transition near 17 K, which is not observed (see Fig. 3). Instead, these features indicate a bulk property is being measured that clearly deviates from strong coupling or BCS weak coupling theory.

After taking the first set of temperature-dependent data (junction #1) the point contact tip was twice mechanically retracted over ~ 100 μm and two new junctions (#2 and #3) were formed on the same sample (*A*), showing the identical spectral shapes and temperature dependence. Since the thread mechanism of the tip approach does not preserve the microscopic lateral position on the sample, these junctions have to be regarded as entirely independent and their consistency thus proves the reproducibility of these observations. In addition it will be shown that *SIS* junctions on sample *B* display nearly identical low-*T* characteristics. Further tests, which included etching of the Au tip, suggested these junctions were formed by breaking off an MgB$_2$ crystal fragment which then forms an *SIS* junction with the bulk material. This procedure of creating *SIS* break junctions is well known for point-contact tunneling into Bi$_2$Sr$_2$CaCu$_2$O$_8$ [10]. The ease with which reproducible *SIS* junctions were formed was quite surprising and this requires us to critically review our previously published data which showed similar spectral shapes at 4.2 K [11], but no *T* dependence was measured. The data presented there were interpreted in terms of *SIN* tunneling with a gap value of 4.3–4.6 meV and no smearing parameter Γ. This analysis is similar in shape to an *SIS* characteristic with $\Delta = 2.5$ meV and $\Gamma = 0.5$ meV (typical parameters used here to fit the data, e.g., in Fig. 2), leading to the possibility that some of the junctions in that work were in fact *SIS* type. This would bring the measured gaps of that work in line with what was consistently observed here.

The values for $\Delta_1(T)$ extracted from the fits to the conductance data on these three junctions are shown in Fig. 3. The uncertainty in the measured gap values is given by the error bars and there is excellent reproducibility among the three junctions. The solid line gives the BCS dependence for a low-temperature gap of 2.5 meV with the expected $T_c = \Delta_1(0)/1.76k_B = 16.5$ K. Comparison of the data with the BCS fit shows a clear anomaly: the small gap persists up to temperatures far beyond the expected T_c. The dashed line gives a *rescaled* BCS $\Delta(T)$ with the T_c adjusted to fit the experimental data. This leads to an extrapolated T_c near the bulk value for MgB$_2$, but we strongly emphasize that there is no basis for this type of rescaling within BCS theory. This should be contrasted with strong-coupling effects which commonly lead to a zero temperature gap that exceeds the BCS value resulting in an

enhanced gap ratio $2\Delta(0)/k_B T_c$. Here, this ratio is much *smaller* than the expected BCS value.

We propose that the data of Fig. 3 together with our analysis of the conductance spectra presented below are compelling evidence of two-band superconductivity as suggested by Liu *et al.* [4]. The absence of any evidence for a second transition in Fig. 3 indicates that Δ_1 is primarily induced via coupling to the 2D band. We believe that the persistent and clear observation of only Δ_1 in our *SIS* and *SIN* junctions is due to the much higher probability of tunneling into the 3D band. This band accounts for 58% of the total DOS [4] which is insufficient to account for its preference. It rather is the dominance of tunneling by electrons with momenta normal to the barrier which favors the 3D band. Assuming a random orientation, there is a relatively low probability of being properly aligned with the 2D band.

The low-temperature conductance spectra reveal a weak but reproducible structure near 9 mV which we believe is related to the large gap, Δ_2, but is not due to direct tunneling into the 2D band. This conclusion is supported by a calculation of the quasiparticle DOS on each sheet using the McMillan tunneling model [7]. This model simulates a coupled, two-band system by including the BCS-type, virtual phonon coupling (pair exchange) between bands [12,13] and also self-energy effects from interband quasiparticle exchange. The model requires the solution of two simultaneous equations:

$$\Delta_1(E) = \frac{\Delta_1^{ph} + \Gamma_1 \Delta_2(E)/\sqrt{\Delta_2^2(E) - (E - i\Gamma_2^*)^2}}{1 + \Gamma_1/\sqrt{\Delta_2^2(E) - (E - i\Gamma_2^*)^2}} \quad (1)$$

for the energy dependence of the two gaps, where the second equation is obtained by interchanging the subscripts 1 and 2. These functions $\Delta_{1,2}(E)$ are subsequently used to compute the DOS in both bands via the usual BCS expression. Convolution of these DOS then yields the desired *SIS* conductance characteristics. The model includes six parameters: the intrinsic pairing gaps on both bands in the absence of any interband coupling, $\Delta_{1,2}^{ph}$, two scattering rates, $\Gamma_{1,2}$, related inversely to the times spent in each band prior to scattering to the other, and two smearing parameters, $\Gamma_{1,2}^*$, which were added to account for lifetime effects within each band. Rather than treat each parameter as free, we fix the intrinsic pairing gaps by considering first principle calculations for MgB$_2$ [4], viz., $\Delta_1^{ph} = 0$ and $\Delta_2^{ph} = 7.2$ meV [14]. The first assumption is further justified by noting that only a single transition is observed in Fig. 3. The observed induced gap magnitude is then adjusted by appropriate choice of $\Gamma_{1,2}$. These parameters are highly interdependent and cannot separately be determined. Good fits can be obtained for ratios Γ_2/Γ_1 between zero and ~ 0.5. We choose 0.25 as representative [15]. The smearing parameters finally are needed to account for the broadening and the in-gap current.
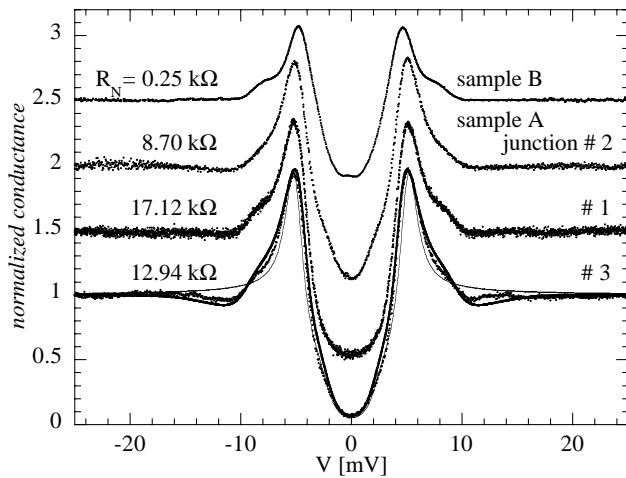
FIG. 4. Low-temperature *SIS* tunneling spectra. The measured data (dots) are normalized to a smooth background. For one set of data the fit (thin solid line) to a small (intrinsic) BCS *s*-wave gap is shown along with a fit (thick solid line) to an induced gap. The parameters used are $\Delta_1^{ph} = 0$, $\Delta_2^{ph} = 7.2$ meV, $\Gamma_1 = 4.0$ meV, $\Gamma_2 = 1.0$ meV, $\Gamma_1^* = 0.5$ meV, and $\Gamma_2^* = 1.0$ meV. See the text for details.

The low-temperature spectra from different junctions on samples *A* and *B* are shown in Fig. 4 to demonstrate the reproducibility of the data. Note that all characteristic features of the data taken on sample *B*, such as the gap magnitude and the additional structure outside the conductance peaks, coincide with those from sample *A*. For one junction (#3), the result of a two-band fit is given along with the BCS model including a smearing of $\Gamma = 0.5$ meV. The BCS fit convincingly reproduces the in-gap conductance and the quasiparticle peak, but it cannot account for the features near 9 mV, which are consistently seen in these *SIS* junctions. The two-band fit is close to the BCS behavior for low bias, but it also reproduces the shoulder and dip at the observed energy in agreement with the data. The higher energy spectral feature is an effect of the large gap, Δ_2, on the quasiparticle self-energy in the 3D band DOS. Note that the dip drops below unity, a characteristic feature of quasiparticle self-energy effects, similar to phonon structures, but which cannot be achieved by arbitrarily adding two BCS DOS from the two bands. The subtlety of the feature near 9 meV, as well as the dip, is more easily understood as an intrinsic feature of the 3D DOS. Our data show no direct contribution from the 2D band [16].

The same formalism used above to calculate the conductances is valid for a proximity sandwich, *P*, consisting of *N* and *S* layers that are coupled by a tunnel barrier *I* [7]; i.e., $P \equiv NIS$. Well-coupled *N* and *S* layers result in spectral features inconsistent with our observations [17]. For $P \equiv NIS$, the small gap in the *N* region has been shown to decrease exponentially with barrier thickness [18]. To explain the small gap of MgB$_2$ as a surface proximity effect (i.e., PIP' for our *SIS* geometry) would produce a noticeable splitting of the zero-bias peak (Fig. 2) unless

the gaps in *P* and P' differed by less than $\sim 20\%$. This is highly unlikely as it would require [18] the tunneling barrier thicknesses in *P* for all MgB$_2$ samples to be within ~ 0.5 Å. Thus it is our *SIS* geometry that allows us to rule out proximity effects.

In conclusion, we have reproducibly observed a small energy gap, $\Delta_1 \sim 2.5$ meV, which smoothly closes near the bulk T_c. This observation, along with a detailed analysis of the conductance spectra, is indicative that MgB$_2$ is an example of the rarely observed phenomenon of two-band superconductivity. While the measured gap values are consistent with the first principles two-band model that assumes pair exchange between bands [4], our spectra are providing strong evidence that interband quasiparticle exchange is important. The data are inconsistent with surface layers of reduced T_c or with proximity effects.

[1] G. Rubio-Bollinger, H. Suderow, and S. Vieira, Phys. Rev. Lett. **86**, 5582 (2001).
[2] F. Giubileo *et al.,* Phys. Rev. Lett. **87**, 177008 (2001).
[3] P. Szabó *et al.,* Phys. Rev. Lett. **87**, 137005 (2001).
[4] A. Y. Liu, I. I. Mazin, and J. Kortus, Phys. Rev. Lett. **87**, 087005 (2001).
[5] J. Kortus *et al.,* Phys. Rev. Lett. **86**, 4656 (2001).
[6] J. M. An and W. E. Pickett, Phys. Rev. Lett. **86**, 4366 (2001).
[7] W. L. McMillan, Phys. Rev. **175**, 537 (1968).
[8] L. Ozyuzer, J. F. Zasadzinski, and K. E. Gray, Cryogenics **38**, 911 (1998).
[9] R. S. Gonnelli *et al.,* Phys. Rev. Lett. **87**, 097001 (2001).
[10] Y. DeWilde *et al.,* Phys. Rev. Lett. **80**, 153 (1998).
[11] H. Schmidt *et al.,* Phys. Rev. B **63**, 220504(R) (2001).
[12] H. Suhl, B. T. Matthias, and L. R. Walker, Phys. Rev. Lett. **3**, 552 (1959).
[13] C. Noce and L. Maritato, Phys. Rev. B **40**, 734 (1989).
[14] The calculated coupling constant $\lambda_B = 0.45$ [4] for the 3D band yields an intrinsic pairing with $T_c < 4.2$ K. It therefore is safe to neglect Δ_1^{ph} for our purpose.
[15] Since $\Gamma_{1,2}$ are interband scattering rates, their ratio is expected to be related to the ratio of the DOS in both bands, N_1/N_2. However, due to the complicated geometry of the Fermi surface, it is not evident to us that all quasiparticles participate in the interband scattering and we therefore do not expect to find $\Gamma_2/\Gamma_1 = N_1/N_2$.
[16] In principle, three channels contribute in parallel to the total current in two-band *SIS* junctions. In the order of increasing tunneling probability, these are 2D-2D, 2D-3D, and 3D-3D, corresponding to quasiparticle peaks at $eV = 2\Delta_2$, $\Delta_1 + \Delta_2$, and $2\Delta_1$. Only the peaks of the dominant 3D-3D spectrum are observed.
[17] G. B. Arnold, Phys. Rev. B **18**, 1076 (1978).
[18] K. E. Gray, Phys. Rev. Lett. **28**, 959 (1972).